ISSN 1063-7850, Technical Physics Letters, 2018, Vol. 44, No. 3, pp. 267–270. © Pleiades Publishing, Ltd., 2018.
Original Russian Text © S.V. Sorokin, I.V. Sedova, K.G. Belyaev, M.V. Rakhlin, M.A. Yagovkina, A.A. Toropov, S.V. Ivanov, 2018, published in Pis'ma v Zhurnal Tekhnicheskoi Fiziki, 2018, Vol. 44, No. 6, pp. 94–102.

Nanoheterostructures with CdTe/ZnMgSeTe Quantum Dots for Single-Photon Emitters Grown by Molecular Beam Epitaxy

S. V. Sorokin*, I. V. Sedova, K. G. Belyaev, M. V. Rakhlin, M. A. Yagovkina, A. A. Toropov, and S. V. Ivanov

Ioffe Physical Technical Institute, Russian Academy of Sciences, St. Petersburg, 194021 Russia

**e-mail: sorokin@beam.ioffe.ru*

Received October 12, 2017

Abstract—Data on the molecular beam epitaxy (MBE) technology, design, and luminescent properties of heterostructures with CdTe/Zn(Mg)(Se)Te quantum dots on InAs(001) substrates are presented. X-ray diffraction has been used to study short-period ZnTe/MgTe/MgSe superlattices used as wide-bandgap barriers in structures with CdTe/ZnTe quantum dots for the effective confinement of holes. It is shown that the design of these superlattices must take into account the replacement of Te atoms by selenium on MgSe/ZnTe and MgTe/MgSe heterointerfaces. Heterostructures with CdTe/Zn(Mg)(Se)Te quantum dots exhibit photoluminescence at temperatures up to 300 K. The spectra of microphotoluminescence at $T = 10$ K display a set of emission lines from separate CdTe/ZnTe quantum dots, the surface density of which is estimated at ~10^{10} cm^{-2}.

DOI: 10.1134/S1063785018030264

In the past two decades, considerable effort has been devoted to the development of high-efficiency single-photon emitters, which are potential sources of radiation for numerous important applications. In particular, these emitters are required in quantum-computation and -telecommunication systems, since they ensure absolute safety of data exchange using quantum-cryptography protocols. A promising approach to the implementation of single-photon emitters is related to the use of semiconductor quantum dots (QDs). The emission of single photons in epitaxial structures with QDs was demonstrated in various systems of A^3B^5 and A^2B^6 compounds, including those with CdSe/Zn(S,Se) [1, 2] and CdTe/ZnTe [3, 4] quantum dots.

A critical parameter favoring the observation of luminescence from single QDs is their low surface density. For example, CdTe/ZnTe quantum dots at low surface density can be obtained by the method of molecular-beam epitaxy (MBE) in the regime of thermal activation (TA). In this case, the formation of QDs is induced by decreasing the surface energy of a strained two-dimensional (2D) CdTe layer through deposition of amorphous Te layer and its subsequent fast desorption [5]. The influence of various parameters (nominal thickness of CdTe quantum dots, and the temperature of their deposition and annealing) of the TA regime on the photoluminescent (PL) properties and density of MBE-grown CdTe/ZnTe quantum dots has been thoroughly studied [5–8]. It was established that the surface density of QDs could be on the order of 10^{10} cm^{-2} [5, 8] and below [6]. Recently [4], we obtained 200-nm-wide mesa structures based on MBA-grown heterostructures with CdTe/ZnTe quantum dots formed in the TA regime, which exhibited the phenomenon of photon antibunching with a mean correlation function value of $g^{(2)}(0) = 0.16$ (± 0.04) at $T = 8$ K (indicative of the single-photon character of PL from the QD). However, increase in the operating temperature of single-photon emitters based on CdTe/ZnTe quantum dots requires using wide-bandgap ZnMgSeTe barriers, which are intended to improve the confinement of holes by increasing valence-band discontinuity at the CdTe/ZnMgSeTe heteroboundary as compared to that for the CdTe/ZnTe interface.

This Letter reports on the MBE growth of nanoheterostructures with CdTe quantum dots incorporated into barriers of quasi-quaternary ZnMgSeTe solid solution in the form of short-period ZnTe/MgTe/MgSe superlattices (SLs) with a period of T_{SL} ~ 2 nm. The structure and PL properties of these nanoheterostructures have been studied. The obtained structures exhibited effective PL from QDs up to room temperature and displayed spectrally resolved emission lines from individual QDs at $T = 10$ K.

The heterostructures with CdTe/Zn(Mg)(Se)Te quantum dots were obtained by pseudomorphous growth on InAs(001) substrates with a 0.2-μm-thick InAs buffer layer in a two-chamber MBE system (SemiTEq Co., Russia) using standard effusion cells with high-purity components (Zn, Cd, Mg, Te) and

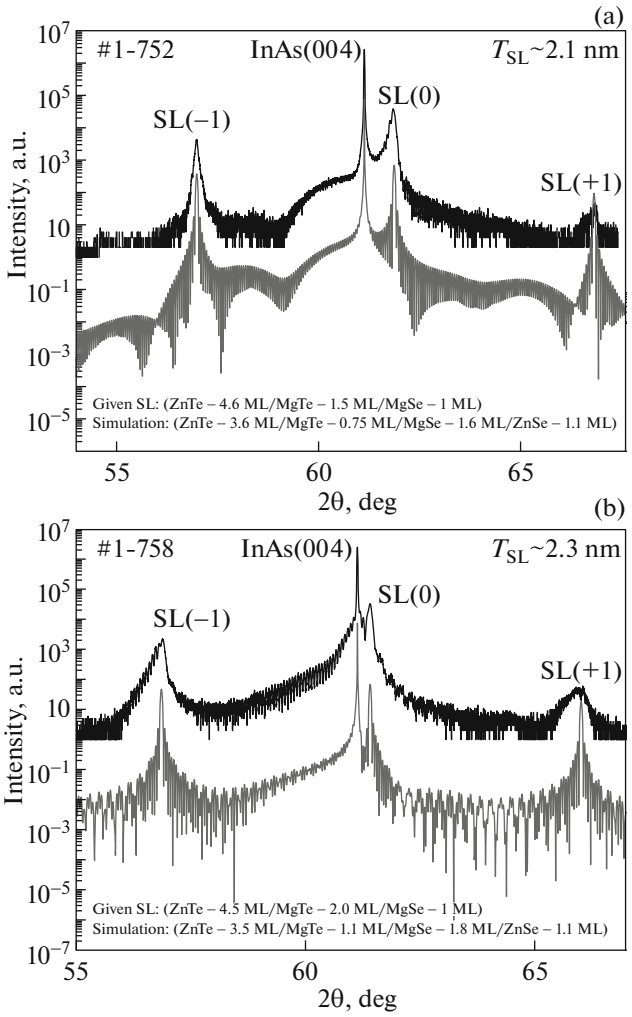

Fig. 1. XRD curves near InAs(004) reflection for (a) a structure with a 0.2-μm-thick ZnTe/MgTe/MgSe superlattice and (b) a structure with CdTe/ZnTe quantum dots confined between barriers representing short-period ZnTe/MgTe/MgSe superlattices. The upper and lower curves correspond to experiment and modeling, respectively.

valve-controlled Se source as molecular-beam generators. The process was carried out at a substrate temperature of $T_S = 295–300$°C. The substrate was heated by the contactless radiative technique. The MBE growth was initiated by simultaneously opening shutters of Zn and Te fluxes toward the surface of InAS buffer layer with (2 × 4)As reconstruction [9]. The growth of CdTe quantum dots was monitored by reflection high-energy electron-diffraction (RHEED) measurements. The structures with CdTe/Zn(Mg)(Se)Te quantum dots comprised a five-monolayer (ML) thick ZnTe seeding layer, an ~150-nm-thick short-period ZnTe/MgTe/MgSe superlattice, a CdTe quantum-dot layer (with nominal CdTe thickness of ~3 ML) separated from SL on both sides with 3-ML ZnTe spacers, and an ~45-nm-thick upper ZnTe/MgTe/MgSe superlattice. The CdTe/ZnTe quantum dots were formed in the TA regime, whereby the increase in T_S upon desorption of the amorphous Te layer was performed in the absence of Te flow to the growth surface [8]. In addition, sample structures containing "blank" ZnTe/MgTe/MgSe superlattices were also prepared.

The as-grown structures were characterized by θ–2θ X-ray-diffraction (XRD) curves in the vicinity of InAs(004) reflection measured on a high-resolution Bruker D8 Discover diffractometer and by transmission electron microscopy (TEM) in the cross-section geometry on a Philips EM-420 instrument. The optical properties of heterostructures with QDs were characterized using PL spectroscopy and low-temperature micro-PL measurements. The PL spectra were recorded using a cooled CCD camera and excitation sources based on laser lines (CUBE lasers, Coherent Inc.) operating at $\lambda = 377$ and 404 nm.

The idea of replacing the quaternary ZnMgSeTe solid solution with short-period SLs of the ZnTe/MgTe/MgSe type was proposed and realized previously [10] for MBE growth of high-reflectivity broadband Bragg's reflectors lattice-matched to ZnTe. The use of SLs significantly simplified control of the growing layer composition by selecting the corresponding thicknesses of binary-compound layers constituting SLs. In the present work, all short-period SLs of the ZnTe/MgTe/MgSe type with an ~2-nm period were grown by MBE in the regime with surface enrichment by a group VI element (Te). The priority of interfacial-layer formation in SLs was determined by differences in the enthalpy of formation of the corresponding binary compounds with zinc-blend (ZB) lattices:

$$\Delta H^0_{298}(\mathrm{MgSe}) > \Delta H^0_{298}(\mathrm{ZnSe}) > \Delta H^0_{298}(\mathrm{MgTe}) > \Delta H^0_{298}(\mathrm{ZnTe})(\mathrm{ZB}). \quad (1)$$

Taking into account relation (1), one can expect the formation of ZnSe layer on the MgSe/ZnTe interface, while the partial replacement of Te atoms by Se atoms at the MgTe/MgSe interface must lead to an increasing MgSe fraction on the SL. These expectations were confirmed by the modeling of θ–2θ XRD curves in the vicinity of InAs(004) reflection for two structures with ZnTe/MgTe/MgSe superlattices (Fig. 1). Good agreement of the experimental and model XRD curves is reached under assumption that ~1.1-ML ZnSe layers are formed at the MgSe/ZnTe interface due to a decrease in the ZnTe layer thickness and an increase in the thickness of MgSe layers by 0.6–0.8 ML at MgTe/MgSe interfaces due to decreasing thickness of adjacent MgTe layers. In addition to the SL period set in modeling of the XRD curves, we also took into account (i) data on the growth rates of binary compounds (SL components) determined from

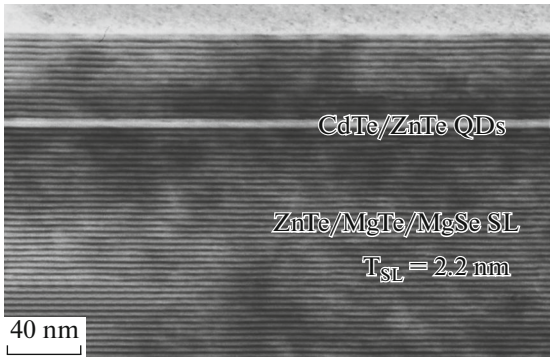

Fig. 2. TEM image of the cross section of a structure with CdTe/ZnTe quantum dots confined between barriers representing short-period ZnTe/MgTe/MgSe superlattices with nominal period $T_{SL} = 2.2$ nm.

intensity oscillations in the RHEED spot and (ii) differences between the growth rates of MgTe and MgSe layers at a constant flux of Mg related to the different lattice periods of these compounds.

The formation of 1.5- and 2.5-ML-thick ZnSe-containing layers on ZnTe/CdSe interfaces during MBE growth of SLs of the ZnTe/CdSe type was previously reported in [11]. However, in contrast to the present work, the ZnTe layers in [11] were grown under Zn-rich conditions. In any case, although the details of the microstructure of interfaces in ZnTe/MgTe/MgSe superlattices are unknown, their contribution should be taken into account in the design of SLs lattice-matched to the InAs substrate.

Figure 2 shows a TEM image of the cross section of a structure with CdTe/ZnTe quantum dots confined between barriers representing short-period ZnTe/MgTe/MgSe superlattices. The image clearly resolves both SL layers and CdTe/ZnTe quantum-dot layers. The SL period amounts to $T_{SL} = 2.2$ nm and slightly differs for the upper and lower SLs, which can be variation of the flows of main components during prolonged interrupt (up to 1.5–2 h, depending on the MBE setup) in the growth that was necessary for decreasing T_S to the temperature (<50°C) of amorphous Te deposition during the formation of CdTe/ZnTe quantum dots in the TA regime. Moreover, a long interruption in growth can lead to the formation of a significant density of stacking faults on the QD/ZnTe interface [12]. At the same time, the TEM image shows complete coherence of the structure with an InAs substrate.

The PL spectra of heterostructures with CdTe/Zn(Mg)(Se)Te quantum dots (Fig. 3) display peaks related to the emission from superlattices and CdTe/ZnTe quantum dots, with the former peak dominating at low temperatures. The spectra clearly reveal a complicated structure of PL from QDs, which begins to predominate at $T > 50$ K. The narrower short-wavelength peak ($E_{max} \sim 2.2$ eV) may be related to emission

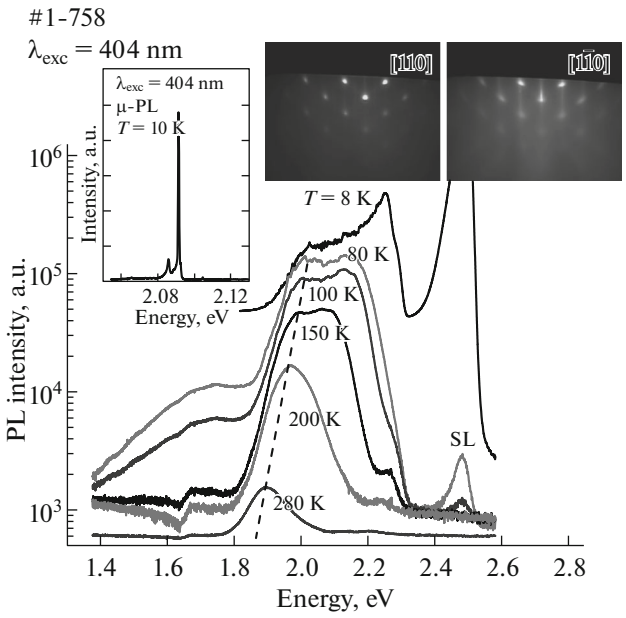

Fig. 3. PL spectra (T = 8–280 K) of the structure with CdTe/ZnTe quantum dots confined between barriers representing short-period ZnTe/MgTe/MgSe superlattices. The insets show (right-hand) RHEED patterns in orthogonal [110] and [1$\bar{1}$0] directions observed during the QD formation and (left) the low-temperature micro-PL spectrum measured under pinhole excitation (T = 10 K).

from the so-called "wetting layer," and the broad long-wavelength peak ($E_{max} \sim 1.9$–2.0 eV) is related to the emission directly from QDs. Due to increased confinement of holes, the PL from QDs is retained up to room temperature. As the temperature grows from T = 8 to 150 K, the PL peak intensity decreases by a factor of 4–5 (against a 25-fold drop for CdTe quantum dots formed in the binary ZnTe barriers).

The formation of CdTe/ZnTe quantum dots is strongly influenced by the residual Se background in the MBE chamber [4, 13]. A significant background pressure of this element in the growth chamber leads to uncontrolled replacement of Te by Se on the CdTe layer surface, which results in both a change in the surface energy and a decrease in the elastic energy, thus hindering QD formation in the TA regime [4]. A radical decrease of Se flux during MBE of MgSe layers at the stage of formation of ZnTe/MgTe/MgSe superlattices allowed the formation of QD to be optimized and the duration of pause with SE source closed to be significantly decreased (this pause is necessary for reducing the Se background in the chamber for the subsequent formation of CdTe quantum dots by MBE in the TA regime). The corresponding RHEED pattern exhibited clear 2D–3D transition in the surface morphology (see right-hand insets to Fig. 3), which was similar to the case of MBE growth of CdTe/ZnTe quantum dots in [8]. The micro-PL spectra (T = 10 K)

of the structure with CdTe/Zn(Mg)(Se)Te quantum dots display a set of narrow discrete emission lines from separate QDs (see the left inset to Fig. 3), the surface density of which is estimated at $\sim 10^{10}$ cm^{-2}.

In concluding, we have used MBE to grow structures with CdTe quantum dots between barriers of quasi-quaternary ZnMgSeTe solid solution in the form of short-period ZnTe/MgTe/MgSe superlattices with an SL period matched to the InAs(001) substrate. The main peculiarities of MBE growth of these SLs related to the spontaneous formation of ZnSe-containing layers on MgSe/ZnTe interfaces and the increase in MgSe fraction in SLs due to the partial replacement of Te atoms by Se atoms on MgTe/MgSe interfaces. It is established that, by decreasing the flux of Se during SL growth it is possible to reduce from several hours to 30 min the duration of pause with the Se source closed upon growth of the lower ZnTe/MgTe/MgSe superlattice. This pause is necessary for eliminating the influence of Se background in the MBE chamber on the formation of CdTe/Zn(Mg)(Se)Te quantum dots in the TA regime. The micro-PL spectra (T = 10 K) of the structure with CdTe/Zn(Mg)(Se)Te quantum dots display a set of narrow discrete emission lines from separate QDs in the spectral range of 2.0–2.2 eV and the surface density of these QDs is estimated at $\sim 10^{10}$ cm^{-2}.

Acknowledgments. We are grateful to A.A. Sitnikova for conducting TEM measurements.

This work was supported by the Russian Science Foundation (project no. 14-22-00107). XRD and TEM investigations were performed at the Center of Collective Use Materials Science and Diagnostics in Advanced Technologies and supported in part by the Ministry of Education and Science of the Russian Federation, agreement no. 14.621.21.0013/28.08.2017, project identifier RFMEFI62117X0018.

REFERENCES

1. A. Tribu, G. Sallen, T. Aichele, R. André, J.-P. Poizat, C. Bougerol, S. Tatarenko, and K. Kheng, Nano Lett. **8**, 4326 (2008).
2. O. Fedorych, C. Kruse, A. Ruban, D. Hommel, G. Bacher, and T. Kümmell, Appl. Phys. Lett. **100**, 061114 (2012).
3. C. Couteau, S. Moehl, F. Tinjod, J. M. Gérard, K. Kheng, H. Mariette, J. A. Gaj, R. Romestain, and J. P. Poizat, Appl. Phys. Lett. **85**, 6251 (2004).
4. S. V. Sorokin, I. V. Sedova, S. V. Gronin, G. V. Klimko, K. G. Belyaev, M. V. Rakhlin, I. S. Mukhin, A. A. Toropov, and S. V. Ivanov, J. Cryst. Growth **477**, 127 (2017).
5. F. Tinjod, B. Gilles, S. Moehl, K. Kheng, and H. Mariette, Appl. Phys. Lett. **82**, 4340 (2003).
6. J. Kobak, J.-G. Rousset, R. Rudniewski, E. Janik, T. Slupinski, P. Kossacki, A. Golnik, and W. Pacuski, J. Cryst. Growth **378**, 274 (2013).
7. P. Wojnar, G. Karczewski, T. Wojtowicz, and J. Kossut, Acta Phys. Polon. A **112**, 283 (2007).
8. S. V. Sorokin, I. V. Sedova, S. V. Gronin, K. G. Belyaev, M. V. Rakhlin, A. A. Toropov, I. S. Mukhin, and S. V. Ivanov, Tech. Phys. Lett. **42**, 1163 (2016).
9. P. Grabs, G. Richter, R. Fiederling, C. R. Becker, W. Ossau, G. Schmidt, L. W. Molenkamp, W. Weigand, E. Umbach, I. V. Sedova, and S. V. Ivanov, Appl. Phys. Lett. **80**, 3766 (2002).
10. W. Pacuski, C. Kruse, S. Figge, and D. Hommel, Appl. Phys. Lett. **94**, 191108 (2009).
11. B. Bonef, L. Gérard, J.-L. Rouviere, A. Grenier, P.-H. Jouneau, E. Bellet-Amalric, H. Mariette, R. André, and C. Bougerol, Appl. Phys. Lett. **106**, 051904 (2015).
12. I. V. Sedova, S. V. Sorokin, A. A. Sitnikova, R. V. Zolotareva, S. V. Ivanov, and P. S. Kop'ev, in *Proceedings of the 7th International Symposium on Nanostructures: Physics and Technology, St. Petersburg, 1999*, p. 547.
13. J.-G. Rousset, J. Kobak, E. Janik, M. Parlinska-Wojtan, T. Slupinski, A. Golnik, P. Kossacki, M. Nawrocki, and W. Pacuski, J. Appl. Phys. **119**, 183105 (2016).

Translated by P. Pozdeev